Journal of Organometallic Chemistry 843 (2017) 62–65

Contents lists available at ScienceDirect

Journal of Organometallic Chemistry

journal homepage: www.elsevier.com/locate/jorganchem

Communication

Ring flipping in heterobimetallic Re-Ir complexes and its effect on structural isomerism: Dynamic NMR and DFT study

Kothanda Rama Pichaandi [a, 1, 2], Lara Kabalan [b, 2], Sabre Kais [a, b], Mahdi M. Abu-Omar [a, *, 1]

[a] Brown Laboratory, Department of Chemistry, Purdue University, 560 Oval Drive, West Lafayette, IN 47907, USA
[b] Qatar Environment and Energy Research Institute, Hamd Bin Khalifa University, Qatar Foundation, PO Box 5825, Doha, Qatar

ARTICLE INFO

Article history:
Received 17 April 2017
Received in revised form
12 May 2017
Accepted 13 May 2017
Available online 17 May 2017

Keywords:
Ring flipping
Bimetallic complex
DFT
Potential energy
Structural isomerism

ABSTRACT

Experimental and DFT study on the ring flipping phenomenon from the two fused puckered five −membered rings in complex [PNP(Me)(CH_3CN)Ir-ReO_3][PF_6] (**2**) and its derivative [PNP(Me)(CN^tBu)Ir-ReO_3][PF_6] (**3**) is reported here. Dynamic NMR studies from $^{31}P\{^1H\}$NMR on ring flipping revealed that complexes **2** and **3** possess $\Delta G^{\ddagger}$ value of 11.2 ± 0.3 and 9.2 ± 0.3 kcal/mol at 298 K respectively. Density Functional Theory (DFT) calculations concurred with the Potential Energy (PE) values of 12.36 and 8.09 kcal/mol respectively for the same phenomena. Also, DFT studies revealed that ring flipping and structural isomerism between **2** and its isomer [PNP(H)Ir-μ(CH_2)-μ(O)-Re$(O)_2$][PF_6] (**1**) possess distinct transition states and can occur concurrently as observed experimentally.

1. Introduction

Pincer metal complexes are widely used in catalytic applications [1–7]. One of their characteristics is ring flipping emanating from the two fused and puckered five−membered rings: one pointing up and another down. This characteristic is explored by Variable-temperature Dynamic NMR spectroscopy (DNMR) [8–11]. Restricting this motion with structurally rigid chiral pincer molecules having no ring flipping character, was realized in asymmetric catalysis [9,12–14]. Classic examples are the report from Nishiyama and coworkers on effective use of this property for asymmetric aldol-type condensation of isocyanides and aldehydes [15,16]. Crabtree and coworkers controlled this motion via outer sphere anion participation in a Pd(II) CCC pincer carbene complex [17]. On the other hand concurrent occurrence of this ring flipping with a structural isomerism is an unusual phenomenon.

We recently reported the synthesis and mechanistic study of the bimetallic complex [PNP(H)Ir-μ(CH_2)-μ(O)-Re$(O)_2$][PF_6] (**1**) and the observation of its structural isomer [PNP(Me)(CH_3CN)Ir-ReO_3][PF_6] (**2**) upon switching the solvent from methylene chloride to acetonitrile (Scheme 1) [18]. From kinetic studies and Density Functional Theory (DFT) calculations we proposed that the structural isomerism of **1** occurs via methyl bridged complex **P**, with the subsequent formation of **S** and then **2** [19]. Interestingly complex **2** and its isocyanide derivative **3** showed ring flipping phenomena on the NMR time scale (Scheme 2). While structures **I** and **III** represent the two atropisomers, structure **II** is the transition state through which the conversion of **I** to **III** takes place. In this report we investigated this ring flipping by DNMR and DFT calculations with the outlook of influencing the structural isomerism from **1** to **2** in the reverse direction.

2. Experimental section

2.1. Computational detail

All the calculations have been carried out with Gaussian 09 [20] code with WB97XD [21,22] functional and three different basis set for better description of the different atoms in the molecule: LanL2DZ [23] which include double- ζ with the Los Alamos effective core applied for Ir and Re, D95(d) [24] basis sets was applied for C, N and O and 6-311G [25] basis set for hydrogen atoms. Structure **3** is taken from single-crystal X-ray diffraction results and structure **2** is taken by replacing the *tert*-butylisocyanide with CH_3CN in **3** [18].

* Corresponding author.
E-mail address: abuomar@chem.ucsb.edu (M.M. Abu-Omar).
[1] Current Address: Department of Chemistry and Biochemistry, University of California, Santa Barbara, CA 93106–9510.
[2] These authors contributed equally.

http://dx.doi.org/10.1016/j.jorganchem.2017.05.030
0022-328X/

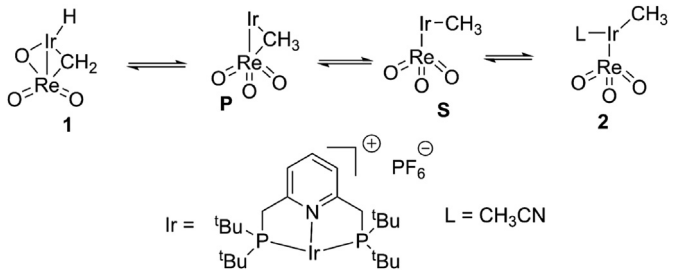

Scheme 1. Structural isomerism observed between complex **1** and **2**.

Structure I and II have C_1 and C_s symmetry respectively. Standard ambient temperature and pressure (298 K at 1 atm) were used in all the simulations that run on gas phase model. PF_6 anion was not included in the calculations.

2.2. Kinetic studies

All reactions were performed in a nitrogen-filled glove box or using standard Schlenk techniques under argon. Solvents were degassed, and purified with a solvent purification system (Pure Process Technology, INC) prior to use. CD_2Cl_2 and CD_3CN were dried over CaH_2, distilled under argon and stored over molecular sieves. All other chemicals were purchased from Aldrich and used as received. One-dimensional NMR spectra were recorded on a Bruker DRX-500 NMR spectrometer equipped with a 5 mm broadband (BBO) probe. Bruker TopSpin software (version 1.3) was used for data acquisition and MestReNova (version 8) was used for processing of NMR spectra. All spectra obtained were referenced to residual solvent peaks accordingly. Complexes **1** and **3** were synthesized following reported literature method [18]. DNMR experiments via $^{31}P\{^1H\}$ NMR were carried out with the temperature range of 210–268 K and 203–268 K for complex **2** and **3** respectively using a mixture of CD_2Cl_2 and CH_3CN in 2:1 ratio. iNMR software was used for simulation of NMR spectra as well as the corresponding rates.

3. Results and discussion

3.1. Dynamic NMR (DNMR) behavior from ring flipping phenomenon in complexes *2* and *3*

Figs. 1 and 2 represent the experimental (left) and simulated (right) $^{31}P\{^1H\}$ NMR spectra of **2** and **3** in the temperature range of 210–268 K and 203 K–268 K representing their DNMR behavior. At lower temperature the $^{31}P\{^1H\}$ showed AB pattern, and as the temperature is raised these signals begin to broaden and approach coalescence at 258 K. In $^1H\{^{31}P\}$ NMR of complex **3** the two AB patterns of protons in the methylidene linker at 203 K approach coalescence at 217 K and become a mono AB pattern (Fig. S2 in

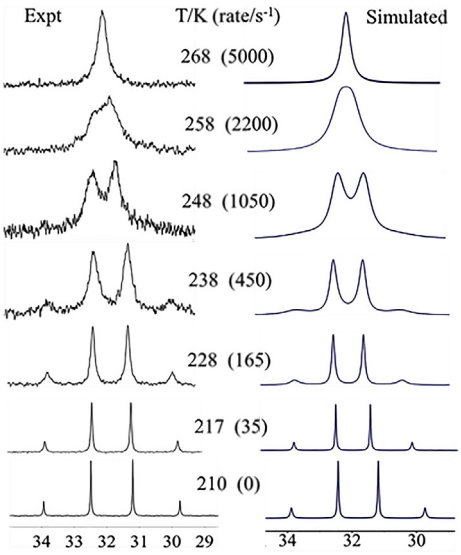

Fig. 1. Experimental (left) and simulated (right) $^{31}P\{^1H\}$NMR spectra of **2** in the temperature range of 210–268 K.

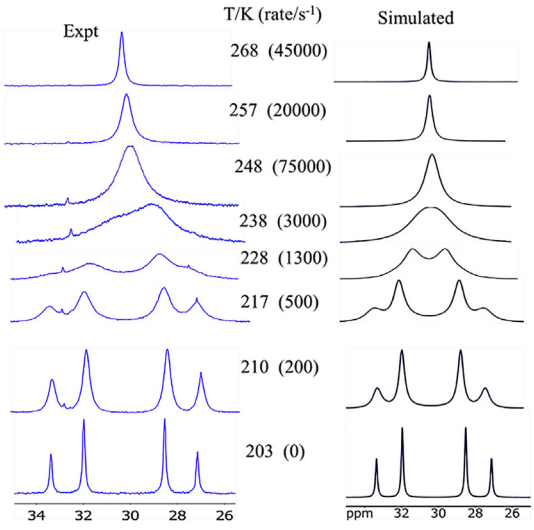

Fig. 2. Experimental (left) and simulated (right) $^{31}P\{^1H\}$ NMR spectra of **3** in the temperature range of 203–268 K.

Supporting Information). However in $^1H\{^{31}P\}$ NMR of complex **2**, this was difficult to observe as the methylidene signals of **1** and **2** appeared in the same region (Fig. S1 in Supporting Information). For DNMR studies $^{31}P\{^1H\}$ NMR was selected for the ease of simulation and line-shape analysis software *iNMR* was used for

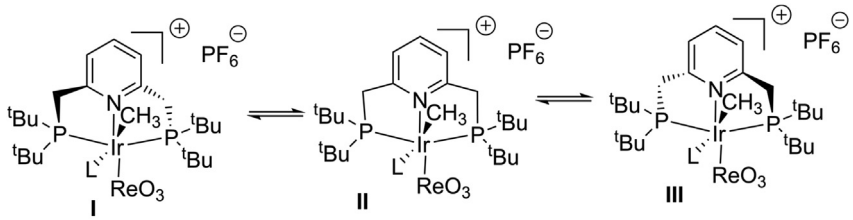

Scheme 2. Ring flipping phenomena observed in complex **2** and **3**.

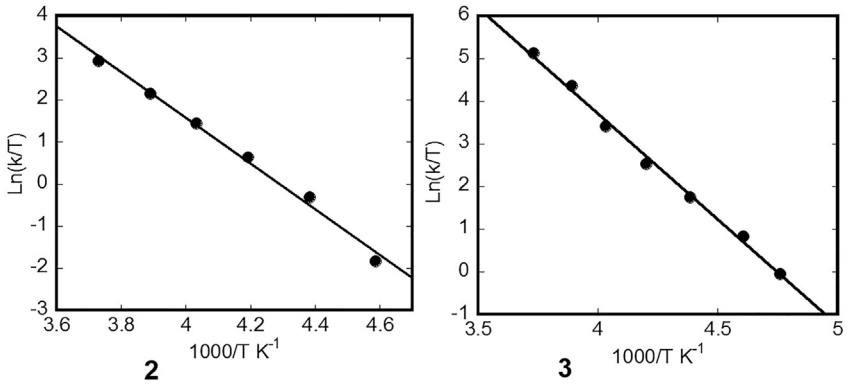

Fig. 3. Eyring plot for ring flipping observed in complex **2** and **3**.

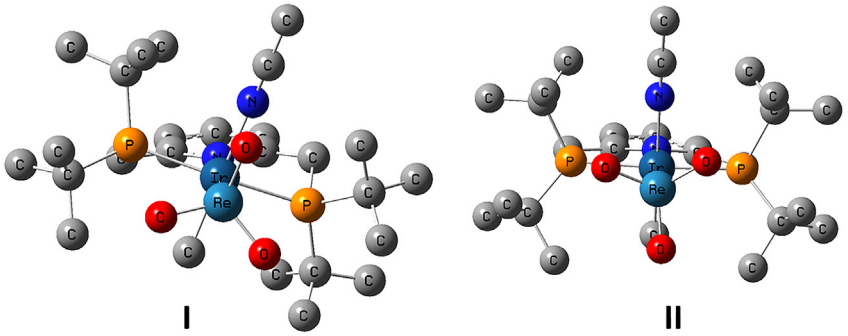

Fig. 4. DFT calculated structures of **I** and **II** for complex **2**. C in grey, N in blue, P in yellow, Ir in light blue, Re in green. H atoms are omitted for clarity. (For interpretation of the references to colour in this figure legend, the reader is referred to the web version of this article.)

simulation of NMR spectra. The k values obtained from the simulation were used to extract the free energies of activation ($\Delta G^{\ddagger}$) using the Eyring relationship (Equation (1)) where *T* is the absolute temperature and *k* is the first-order rate constant in s^{-1}

$$\ln\left(k_{\psi}/T\right) = -\Delta H^{\ddagger}/RT + \ln\left(k_B/h\right) + \Delta S^{\ddagger}/R \qquad (1)$$

Eyring plots for **2** and **3** are presented in Fig. 3. Both complexes **2** and **3** possess similar $\Delta G^{\ddagger}$ value of 11.2 ± 0.3 and 9.2 ± 0.3 kcal/mol at 298 K respectively, and these values are consistent with the literature for ring flipping phenomena for analogous pincer complexes [10,17].

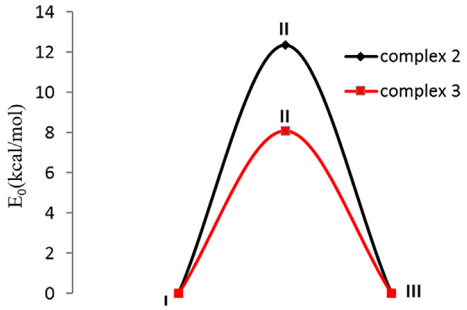

Fig. 5. PE diagram for the ring flipping in complex **2** and **3**.

3.2. DFT study

Mazzanti and co-workers reported in a review on ring flipping that the total energies of different states obtained from DFT give the best fits with experimentally acquired DNMR spectroscopic data, hence we followed their strategy.[9] DFT calculations were carried out at WB97XD/LanL2DZ, D95(d) and 6–311 G level by comparing the structures **I** with **II** (Scheme 2) of complexes **2** and **3**. Structure **III** was an atropisomer of structure **I** and was considered to have the same energy as **I**. Structure **I** was a global minimum structure and structure **II** was obtained as transition state (Fig. 4 represent **2** and supporting information for **3**). For complex **2** the energy difference between **I** to **II** is equal to 12.33 kcal/mol while it is 8.09 kcal/mol for complex **3** (Fig. 5). Both are in good agreement with experimental $\Delta G^{\ddagger}$ values (11.2 ± 0.3 and 9.2 ± 0.3 kcal/mol, respectively).

Next we looked into the possibility of the observed ring flipping, influencing the structural isomerization between **1** and **2**. In our earlier report [19] removal of acetonitrile from **2** resulted the intermediate **S** (first step in the reverse direction of **1** to **2** in Scheme 1) and the PE barrier for this step is 12.3 kcal/mol. This inferences that the decrease in degree of coordination of acetonitrile to the iridium metal center in **2** favors the formation of **S**.

If the ring flipping has any influence on structural isomerism, it has to be in the form of N(CH_3CN)–Ir bond distance elongation. Therefore, we compared the bond distance of N(CH_3CN)–Ir in **I** and **II**. Interestingly structure **II** has longer (0.026 Å) nitrogen to iridium bond distance than **I** indicating that the acetonitrile coordination in complex **2** becomes weaker during ring flipping. Also, the PE barrier of 12.3 kcal/mol for the transformation **2** to **S** is comparable to that for ring flipping (12.36 kcal/mol). Hence we investigated the feasibility of **II** being the same transition state for both ring flipping as well as conversion of **2** to **S**. However a scan with the increase of the Ir–N≡C–CH_3 bond distance in transition state structure **II** first resulted in **I** before transforming to **S**, requiring another transition state (TS*) as has been described in our earlier report (Fig. 6) [19]. This finding implies that ring flipping and the transformation of **2** to **S** follow different pathways with distinct transition states and thereby are independent.

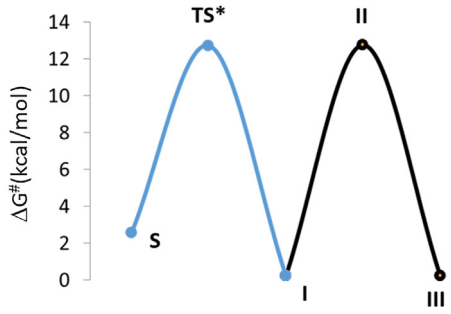

Fig. 6. PE diagram representing the two independent pathways for ring flipping (black line) and the conversion of **2** to **S** (blue line: the first step in the reverse direction of structural isomerism of **1** to **2**). (For interpretation of the references to colour in this figure legend, the reader is referred to the web version of this article.)

4. Conclusion

We established the ring flipping phenomena from the two fused puckered five–membered rings in the Re-Ir complexes **2** and **3** by DNMR experiments and supported by DFT calculations. In both complexes **2** and **3**, the experimental PE values of 11.2 ± 0.3 and 9.2 ± 0.3 kcal/mol concurs with DFT values of 12.33 and 8.09 kcal/mol, respectively. Furthermore, DFT studies revealed that the transition state involved in ring flipping is different than the one observed in conversion of **2** to **S**. Hence ring flipping and structural isomerism observed in complex **2** are independent and can occur concurrently as has been observed experimentally.

Supporting materials

VT $^{1}H\{^{31}P\}$ NMR of complex **2** and **3**, DFT figures for complex **3** and xyz coordinates of structures of **I** and **II** of complex **2** and **3** are supplied as Supporting Information and this material is available free of charge via the Internet at http://www.sciencedirect.com.

Author contributions

The manuscript was written through contributions of all authors. All authors have given approval to the final version of the manuscript.

Funding sources

Funding for this research was provided by DOE-BES, Grant no. DE-FG-02-06ER15794 and Qatar National Research Foundation (QNRF), Grant no. NPRP 6-370-1-075.

Acknowledgment

We thank Dr. Huaping Mo Purdue University for helping us with the NMR experiments. We are extremely grateful for the Research Computing Center in Texas A&M University at Qatar where the calculations were conducted.

Appendix A. Supplementary data

Supplementary data related to this chapter can be found at http://dx.doi.org/10.1016/j.jorganchem.2017.05.030.

References

[1] K. J. Szabó, O. F. Wendt, in, Wiley-VCH Verlag GmbH & Co. KGaA, 2014, pp. 1–302.
[2] G.R.G. Freeman, G.R.J.A.G. Williams, Metal complexes of pincer ligands: excited states, photochemistry, and luminescence, Organomet. Pincer Chem. 40 (2013) 89–130, http://dx.doi.org/10.1007/978-3-642-31081-2_4.
[3] C. Gunanathan, D. Milstein, Catalysis by pincer complexes: synthesis of esters, amides, and peptides, in: Pincer and Pincer-type Complexes, Wiley-VCH Verlag GmbH & Co. KGaA, 2014, pp. 1–30.
[4] S. Werkmeister, J. Neumann, K. Junge, M. Beller, Pincer-type complexes for catalytic (De)hydrogenation and transfer (De)hydrogenation reactions: recent progress, Chem. Euro. J. 21 (2015) 12226–12250.
[5] S. Chakraborty, P. Bhattacharya, H. Dai, H. Guan, Nickel and iron pincer complexes as catalysts for the reduction of carbonyl compounds, Acc. Chem. Res. 48 (2015) 1995–2003.
[6] J. Choi, A.H.R. MacArthur, M. Brookhart, A.S. Goldman, Dehydrogenation and related reactions catalyzed by iridium pincer complexes, Chem. Rev. 111 (2011) 1761–1779.
[7] C. Gunanathan, D. Milstein, in: T. Ikariya, M. Shibasaki (Eds.), Top. Organomet. Chem, Springer, Berlin/Heidelberg, 2011, pp. 55–84.
[8] A. Mazzanti, M. Chiarucci, K.W. Bentley, C. Wolf, Computational and DNMR investigation of the isomerism and stereodynamics of the 2,2′-binaphthalene-1,1′-diol scaffold, J. Org. Chem. 79 (2014) 3725–3730.
[9] L. Ma, P.M. Imbesi, J.B. Updegraff, A.D. Hunter, J.D. Protasiewicz, Synthesis and structural studies of NCN diimine palladium pincer complexes bearing m-terphenyl scaffolds, Inorg. Chem. 46 (2007) 5220–5228.
[10] D. Casarini, L. Lunazzi, A. Mazzanti, Recent advances in stereodynamics and conformational analysis by dynamic NMR and theoretical calculations, Euro. J. Org. Chem. 2010 (2010) 2035–2056.
[11] A. Mazzanti, D. Casarini, in: Wiley Interdisciplinary Reviews: Computational Molecular Science, John Wiley & Sons, Inc., 2012, pp. 613–641.
[12] K. Takenaka, M. Minakawa, Y. Uozumi, NCN pincer palladium complexes: their preparation via a ligand introduction route and their catalytic properties, J. Am. Chem. Soc. 127 (2005) 12273–12281.
[13] R.E. Andrew, D.W. Ferdani, C.A. Ohlin, A.B. Chaplin, Coordination induced atropisomerism in an NHC-based rhodium macrocycle, Organometallics 34 (2015) 913–917.
[14] E. Peris, R.H. Crabtree, Recent homogeneous catalytic applications of chelate and pincer N-heterocyclic carbenes, Coord. Chem. Rev. 248 (2004) 2239–2246.
[15] Y. Motoyama, H. Kawakami, K. Shimozono, K. Aoki, H. Nishiyama, Synthesis and X-ray crystal structures of bis(oxazolinyl)phenyl-derived chiral palladium(II) and platinum(II) and -(IV) complexes and their use in the catalytic asymmetric aldol-type condensation of isocyanides and aldehydes, Organometallics 21 (2002) 3408–3416.
[16] J.M. Longmire, X. Zhang, M. Shang, Synthesis and X-ray crystal structures of palladium(II) and platinum(II) complexes of the PCP-type chiral tridentate ligand (1R,1′R)-1,3-bis[1-(diphenylphosphino)ethyl]benzene. Use in the asymmetric aldol reaction of methyl isocyanoacetate and aldehydes, Organometallics 17 (1998) 4374–4379.
[17] J.R. Miecznikowski, S. Grundemann, M. Albrecht, C. Megret, E. Clot, J.W. Faller, O. Eisenstein, R.H. Crabtree, Outer sphere anion participation can modify the mechanism for conformer interconversion in Pd pincer complexes, Dalton Trans. (2003) 831–838.
[18] K.R. Pichaandi, P.E. Fanwick, M.M. Abu-Omar, C–H activation of methyltrioxorhenium by pincer iridium hydride to give agile Ir-Re bimetallic compounds, Organometallics 33 (2014) 5089–5092.
[19] K.R. Pichaandi, L. Kabalan, S. Kais, M.M. Abu-Omar, Mechanism of isomerization and methyl migration in heterobimetallic Rhenium-Iridium complexes: experimental and DFT study, Organometallics 35 (2016) 605–611.
[20] M. J. Frisch, G. W. Trucks, H. B. Schlegel, G. E. Scuseria, M. A. Robb, J. R. Cheeseman, G. Scalmani, V. Barone, B. Mennucci, G. A. Petersson, H. Nakatsuji, M. Caricato, X. Li, H. P. Hratchian, A. F. Izmaylov, J. Bloino, G. Zheng, J. L. Sonnenberg, M. Hada, M. Ehara, K. Toyota, R. Fukuda, J. Hasegawa, M. Ishida, T. Nakajima, Y. Honda, O. Kitao, H. Nakai, T. Vreven, J. J. A. Montgomery, J. E. Peralta, F. Ogliaro, M. Bearpark, J. J. Heyd, E. Brothers, K. N. Kudin, V. N. Staroverov, T. Keith, R. Kobayashi, J. Normand, K. Raghavachari, A. Rendell, J. C. Burant, S. S. Iyengar, J. Tomasi, M. Cossi, N. Rega, J. M. Millam, M. Klene, J. E. Knox, J. B. Cross, V. Bakken, C. Adamo, J. Jaramillo, R. Gomperts, R. E. Stratmann, O. Yazyev, A. J. Austin, R. Cammi, C. Pomelli, J. W. Ochterski, R. L. Martin, K. Morokuma, V. G. Zakrzewski, G. A. Voth, P. Salvador, J. J. Dannenberg, S. Dapprich, A. D. Daniels, O. Farkas, J. B. Foresman, J. V. Ortiz, J. Cioslowski, D. J. Fox, Gaussian, Inc., Wallingford CT, (2009).
[21] J.-D. Chai, M. Head-Gordon, Long-range corrected hybrid density functionals with damped atom-atom dispersion corrections, Phys. Chem. Chem. Phys. 10 (2008) 6615–6620.
[22] J.-D. Chai, M. Head-Gordon, Systematic optimization of long-range corrected hybrid density functionals, J. Chem. Phys. 128 (2008) 084106.
[23] P.J. Hay, W.R. Wadt, Ab initio effective core potentials for molecular calculations. Potentials for K to Au including the outermost core orbitals, J. Chem. Phys. 82 (1985) 299–310.
[24] T. H. Dunning, P. J. Hay, in: H.F. Schaefer (Ed.), Plenum, New York, 1976, pp. 1–28.
[25] R. Krishnan, J.S. Binkley, R. Seeger, J.A. Pople, Self-consistent molecular orbital methods. XX. A basis set for correlated wave functions, J. Chem. Phys. 72 (1980) 650–654.